Chemical Geology, 40 (1983) 25—42
Elsevier Science Publishers B.V., Amsterdam · Printed in The Netherlands

MANGANITE FORMATION IN THE FIRST STAGE OF THE LATERITIC MANGANESE ORES IN AFRICA

DANIEL NAHON[1], ANICET BEAUVAIS[1], JEAN-LOUP BOEGLIN[2], JACQUES DUCLOUX[1] and PACOME NZIENGUI-MAPANGOU[3]

[1] *Laboratoire de Pétrologie de la Surface, E.R.A. 220, Université de Poitiers, 86022 Poitiers Cedex (France)*
[2] *Office Recherche Scientifique et Technique Outre Mer, Paris (France)*
[3] *COMILOG, Service Prospections Extérieures, Moanda (Gabon)*

(Received June 23, 1982; revised and accepted November 25, 1982)

ABSTRACT

Nahon, D., Beauvais, A., Boeglin, J.-L., Ducloux, J. and Nziengui-Mapangou, P., 1983. Manganite formation in the first stage of the lateritic manganese ores in Africa. Chem. Geol., 40: 25—42.

Lateritic profiles on manganiferous rocks from two areas in central West Africa permit the observation of manganite formation on rocks of different primary nature. In an area of gondites and tephroitites (Ziemougoula, Ivory Coast) manganites are found to replace tephroites and manganocalcites, whereas in a weathered carbonate sequence (Moanda, Gabon) manganite replaces rhodochrosite. In both areas manganite occurrence is limited to a very narrow and basal portion of the altered profile, in conformity with the limited stability field established for this mineral. It is found that manganites of different mineral lineages may be distinguished chemically from one another by variation in the ratio MnO/(CaO + MgO).

INTRODUCTION

The Lateritic weathering of manganese-bearing rocks was studied in tropical and equatorial Africa. Two areas were especially studied. The first one was near Ziemougoula in the northwest of Ivory Coast, where a thick weathered cover develops at the expense of a Birrimian metamorphic parent-rock made up of gondites and tephroitites. The second is the minefield of Moanda in Gabon where the weathering profile overlies Precambrian, unmetamorphosed calcareous shales. Thus, the genesis of manganite in rocks of diverse origins and mineralogy has been studied under similar regimes of lateritic alteration. This permits an examination of the influence of parent-rock composition on the secondary manganite phases and provides an opportunity to circumscribe and differentiate manganites of different parageneses.

0009-2541/83/$03.00

MANGANITE FORMATION IN WEATHERING PROFILES OF ZIEMOUGOULA (IVORY COAST)

The Birrimian metamorphic parent rocks consist essentially of 65% tephroite, 20% spessartite garnet and 10% manganocalcite. The remaining 5% are manganese-bearing chlorites and sulphides. These minerals respond differently to weathering. Thus, at the base of weathering profiles, spessartites are unweathered during the transformation of tephroite, manganocalcite and chlorite. These latter minerals weather into Mn-oxyhydroxides at the earliest stages, but garnet weathers higher in the profile, in a zone where these first Mn-oxyhydroxides are replaced by secondary Mn-oxides. In this paper we deal only with the first transformation of tephroite, manganocalcite into manganite. Chlorite is replaced by a mixture of Mn-oxyhydroxide + kaolinite.

Parent-minerals

Tephroite crystals are anhedral and tightly cemented into a fine-grained mosaic. The chemical compositions obtained by means of the microprobe (Table I) yield the following average formula for the tephroite:

$$[(Si_{0.99}\ Al_{0.01})\ O_4]\ [Cr^{3+}{}_{0.001}\ Fe^{2+}{}_{0.010} Mn_{1.846} Mg_{0.136} Ca_{0.007}]$$

Nests of chlorite appear at the grain junctions of tephroite crystals, and from their compositions (Table II) we can note the following average formula for chlorite:

$$[(Si_{3.017} Al_{0.983})\ O_{10}]\ [Al_{1.068}\ Fe_{0.067}\ Mn_{0.680}\ Mg_{4.140}\ Ca_{0.002})\ (OH)_8]$$

The manganocalcite evolves in patches which can locally replace the border of other parent-minerals. Thus, the manganocalcite appears as the last

TABLE I

Chemical compositions of tephroites

	Sample No.					Average
	1	*2*	*3*	*4*	*5*	
SiO_2	30.22	29.95	30.43	30.01	30.69	30.26
Al_2O_3	0.27	0.43	0.12	0.33	0.21	0.27
Fe_2O_3	—	—	—	—	—	—
Cr_2O_3	0.08	0.01	0.08	0.01	0.01	0.04
FeO	0.48	0.73	0.03	0.60	0.03	0.37
MnO	66.18	66.07	66.64	66.72	66.25	66.37
MgO	2.43	3.48	2.47	2.85	2.51	2.75
CaO	0.15	0.20	0.15	0.20	0.27	0.19
Total	99.81	100.87	99.92	100.72	99.97	100.25

TABLE II

Chemical compositions of chlorites

	Sample No.								Average
	1	*2*	*3*	*4*	*5*	*6*	*7*	*8*	
SiO_2	31.09	32.68	31.25	31.11	30.53	33.40	30.98	30.54	31.45
Al_2O_3	17.68	17.60	17.98	17.96	17.60	18.71	18.23	19.39	18.14
Fe_2O_3	n.d.	n.d.	n.d.	n.d.	n.d.	n.d.	n.d.	n.d.	n.d.
Cr_2O_3	—	—	—	—	—	—	—	—	—
FeO	0.51	0.93	1.21	1.09	1.18	0.43	0.98	0.31	0.83
MnO	7.78	8.10	8.51	8.50	8.27	8.28	8.25	9.27	8.37
MgO	29.81	28.40	30.16	29.05	28.85	27.19	30.04	28.27	28.97
CaO	—	0.02	0.02	—	0.04	0.13	—	—	0.02
Na_2O	n.d.	n.d.	n.d.	n.d.	n.d.	n.d.	n.d.	n.d.	n.d.
K_2O	—	0.02	—	—	—	—	0.03	—	—
TiO_2	—	—	—	—	—	—	—	—	—
CoO	—	0.13	—	—	—	—	—	0.04	0.02
NiO	—	—	0.21	0.06	0.05	0.11	—	—	0.05
CuO	0.14	—	—	0.09	0.10	—	—	0.03	0.04
ZnO	0.27	—	—	—	0.04	—	0.80	—	0.14
H_2O*	12.72	12.12	10.66	12.14	13.34	11.75	10.69	12.15	11.97
Total	100.00	100.00	100.00	100.00	100.00	100.00	100.00	100.00	100.00

*Obtained by difference.
n.d. = not determined; — = beyond detection limit.

TABLE III

Chemical compositions of manganocalcite

	Sample No.						Average
	1	*2*	*3*	*4*	*5*	*6*	
SiO_2	0.05	—	0.01	0.05	0.01	—	0.12
Al_2O_3	—	—	—	0.03	0.01	—	—
Fe_2O_3	—	—	—	—	—	—	—
Cr_2O_3	—	0.07	—	0.07	—	—	0.02
FeO	0.04	0.10	—	—	0.04	0.12	0.05
MnO	15.50	11.84	16.63	10.87	13.00	11.48	13.22
MgO	0.34	0.14	0.36	0.21	0.26	0.20	0.25
CaO	47.49	49.88	42.99	51.02	48.24	49.84	48.24
Na_2O	n.d.	n.d.	n.d.	n.d.	n.d.	n.d.	n.d.
K_2O	0.02	0.01	—	—	—	—	—
TiO_2	—	—	—	—	0.02	0.11	0.02
CoO	—	—	0.07	—	0.13	0.19	0.06
CO_2*	36.56	37.96	39.94	37.75	38.29	38.06	38.12
Total	100.00	100.00	100.00	100.00	100.00	100.00	100.00

*Obtained by difference.
n.d. = not determined; — = beyond detection limit.

PLATE I

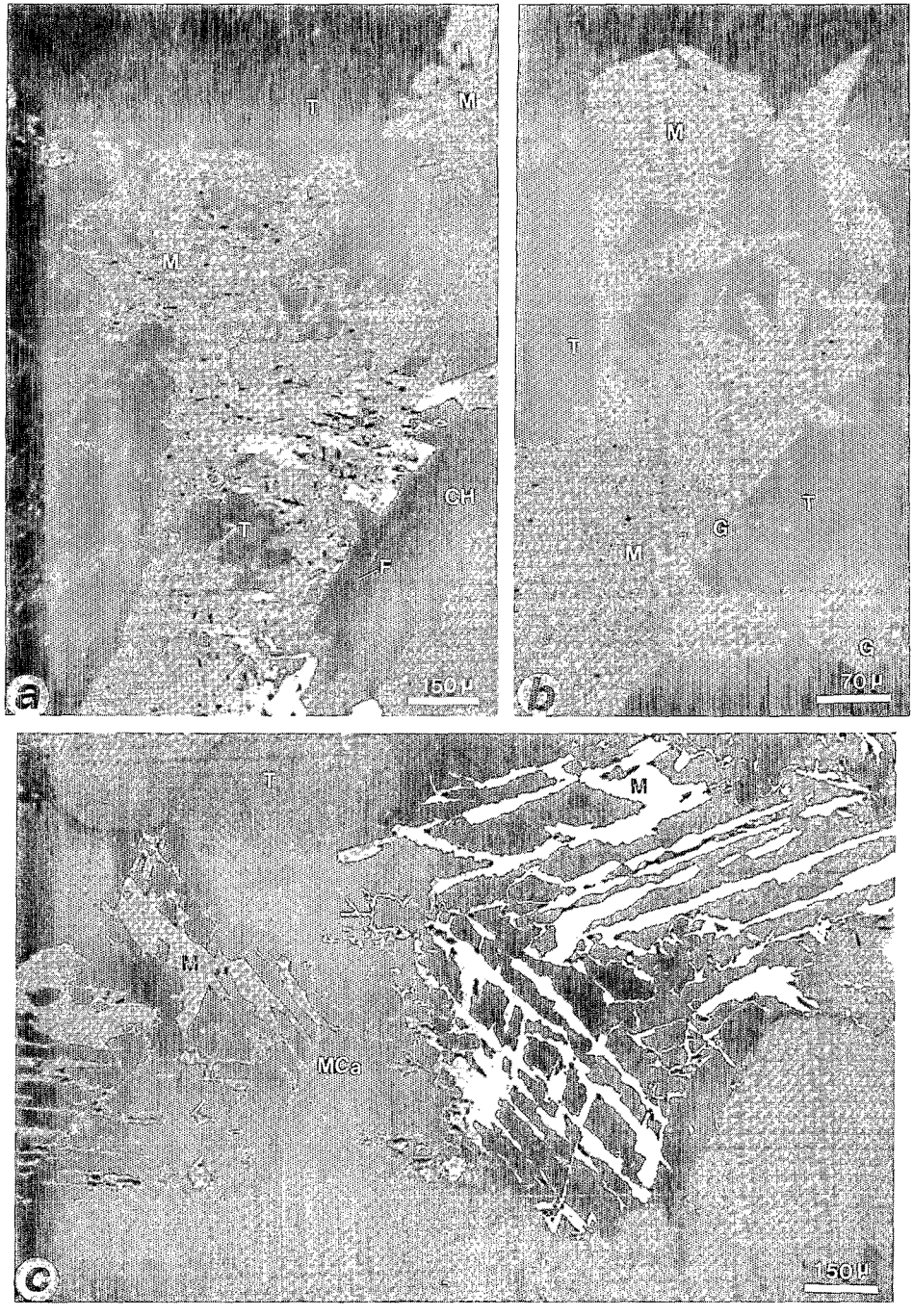

crystallized phase of the parent-rock. Here too, chemical compositions were obtained by means of the electron microprobe and are reported in Table III. The average formula, calculated on the basis of two oxygens, is

$(Ca_{1.634}\, Mn^{2+}{}_{0.354}\, Mg_{0.012})\, (CO_3)_2$

Transformation of tephroite into manganite

In some pits we have noted an ephemeral weathering of tephroite into Mn^{2+}-smectites (Nahon et al., 1982) which precede the manganite stage. But generally the manganite appears as the first product of the replacement of

TABLE IV

Chemical compositions of manganite crystals generated from tephroites

	Sample No.							Average
	1	*2*	*3*	*4*	*5*	*6*	*7*	
SiO_2	4.02	2.74	2.27	3.01	1.84	2.81	2.15	2.69
Al_2O_3	—	—	0.03	0.12	—	0.04	—	0.03
Fe_2O_3	—	—	—	0.28	0.09	0.33	—	0.10
Cr_2O_3	—	—	—	—	0.03	—	—	—
Mn_2O_3	84.52	84.30	85.22	83.08	84.63	85.43	85.70	84.70
CO_2O_3	—	—	—	0.25	0.23	—	—	0.07
FeO	—	—	—	—	—	—	—	—
MgO	—	0.02	0.03	0.12	0.01	0.02	—	0.03
CaO	0.15	0.32	0.06	0.36	0.15	0.11	0.10	0.18
Na_2O	n.d.	n.d.	n.d.	n.d.	n.d.	n.d.	n.d.	n.d.
K_2O	—	0.02	—	0.01	—	—	—	—
TiO_2	—	—	—	—	—	—	—	—
H_2O*	11.31	12.60	12.39	12.77	13.02	11.26	12.05	12.21
Total	100.00	100.00	100.00	100.00	100.00	100.00	100.00	100.00

*Obtained by difference.
n.d. = not determined; — = beyond detection limit.

PLATE I

Manganite formation in weathering profiles of Ziemougoula (Ivory Coast).

a. Transformation of tephroite into manganite: *T* = tephroite; *M* = mosaic of euhedral manganite crystals (one can note tephroite relict among manganite crystals); *CH* = chlorite; *F* = microfissures from opening-up and buckling of the chlorite lamellae. Thin section under crossed polarizers.

b. Details of manganite crystals: *M* = manganite crystals; *T* = tephroite; *G* = unweathered spessartite garnet. Thin section under crossed polarizers.

c. Transformation of manganocalcite into manganite: *MCa* = manganocalcite; *M* = manganite crystals developed from cleavages; *T* = tephroite. Thin section in plain light.

tephroite. These modifications begin in microfissures traversing tephroite crystals and develop as a mosaic of euhedral manganite crystals easily recognized under reflected light (Plate I, a and b). Table IV gives the chemical compositions obtained on such manganite with the electron microprobe.

One can note that silica is not entirely leached when manganite appears. The irregular distribution of silica among manganite crystals suggests a scattering of microconcretions of SiO_2. In addition, the distribution pattern of Si shows that silica is more abundant near the edges of unweathered tephroite.

Transformation of manganocalcite into manganite

A well-crystallized manganite mosaic develops from cross-cleavages and microfractures towards unweathered manganocalcite (Plate I, C). These manganite crystals are similar, under reflected light, to those observed in the weathering products of tephroite.

With the advance of weathering, the manganite develops at the expense of manganocalcite, eventually isolating residual fragments of the parent-carbonate. Each fragment retains the crystallographic orientation of the original carbonate. This proves the in situ weathering of manganocalcite.

The compositions of these manganite crystals (Table V) compared to those of manganocalcite (Table III) enlightens us regarding the source of the silica impurities. As the parent-manganocalcite is almost depleted in this element, we can consider a silica pollution from the surrounding tephroites which weather at the same time as manganocalcite.

Manganite crystallized in fissures

Many fissures cross the rock and cut each parent-mineral and its weathering product. These fissures are ~ 1 mm thick and are covered or filled by manganite crystals which are perpendicular to the walls. Under the microscope these crystals present optical features similar to those observed in weathering products of tephroite or manganocalcite, though they are larger in size. Their compositions are given in Table VI. One can note that these manganite crystals are the richest in Mn.

X-ray characterization of Ziemougoula manganite

The manganite phase was separated by hand-picking from crushed weathered rocks, analysed by X-ray diffraction (XRD) and infra-red (IR) spectrometry. We could not, however, differentiate manganite crystals originating from tephroite from those of manganocalcite or from fissures. X-ray patterns obtained are compared to ASTM data, and crystallographic parameters are calculated by the UNIT-CELL program (Table VII). We can note a slight difference between the parameters of standard manganite and the manganite phase of Ziemougoula.

TABLE V

Chemical compositions of manganite crystals generated from manganocalcite

	Sample No.														Average
	1	*2*	*3*	*4*	*5*	*6*	*7*	*8*	*9*	*10*	*11*	*12*	*13*	*14*	
SiO_2	0.35	0.48	0.42	0.67	0.37	0.57	0.35	0.37	0.43	0.88	0.31	0.39	0.49	0.29	0.45
Al_2O_3	0.02	—	—	0.01	—	0.03	0.01	0.02	0.04	0.05	—	—	0.06	—	0.02
Fe_2O_3	0.04	0.29	—	—	0.08	—	0.01	—	—	0.21	—	0.15	0.14	0.25	0.08
Cr_2O_3	—	0.05	0.01	—	—	0.01	0.01	—	—	—	—	—	0.07	—	0.01
Mn_2O_3	74.69	74.03	73.53	73.76	75.76	74.64	74.08	68.35	68.58	70.18	70.38	68.67	70.98	75.26	72.36
CO_2O_3	0.32	0.19	0.23	0.01	0.40	0.01	0.11	0.02	—	—	0.21	0.02	0.31	0.46	0.16
FeO	—	—	—	—	—	—	—	—	—	—	—	—	—	—	—
MgO	0.65	0.56	0.47	0.61	0.51	0.56	0.63	0.51	0.06	0.59	0.52	0.56	0.61	1.02	0.56
CaO	5.32	5.19	5.12	5.59	4.75	5.62	5.22	5.53	5.58	5.57	5.77	5.85	5.47	4.54	5.36
Na_2O	0.08	—	—	0.02	—	0.04	0.07	n.d.	n.d.	n.d.	n.d.	n.d.	n.d.	n.d.	0.03
K_2O	—	—	0.07	0.05	—	0.04	—	0.10	0.07	0.07	0.02	0.03	0.02	0.01	0.03
TiO_2	—	—	—	—	—	—	—	—	—	0.04	—	—	—	—	—
H_2O*	18.53	19.21	20.15	19.28	18.13	18.48	19.51	25.10	25.24	22.41	22.79	24.33	21.85	18.17	20.96
Total	100.00	100.00	100.00	100.00	100.00	100.00	100.00	100.00	100.00	100.00	100.00	100.00	100.00	100.00	100.00

*Obtained by difference.

n.d. = not determined; — = beyond detection limit.

TABLE VI

Chemical compositions of manganite crystals from cracks and fissures

	Sample No.							Average
	1	*2*	*3*	*4*	*5*	*6*	*7*	
SiO_2	1.58	1.51	1.11	1.69	1.24	0.95	1.45	1.36
Al_2O_3	0.04	0.01	0.09	—	0.08	0.05	0.03	0.04
Fe_2O_3	0.24	0.28	0.21	0.12	0.12	—	—	0.14
Cr_2O_3	—	—	0.09	—	—	0.05	—	0;02
Mn_2O_3	85.49	84.97	84.83	85.54	83.87	87.23	86.52	85.49
Co_2O_3	0.08	0.09	—	0.21	0.18	0.03	0.13	0.10
FeO	—	—	—	—	—	—	—	—
MgO	—	0.04	—	—	0.05	—	0.04	0.02
CaO	0.01	—	—	—	—	—	—	—
Na_2O	n.d.	n.d.	n.d.	n.d.	n.d.	n.d.	n.d.	n.d.
K_2O	—	—	—	—	—	—	—	—
TiO_2	—	—	—	0.01	—	—	—	—
CuO	—	—	—	0.13	—	0.05	0.19	0.05
ZnO	0.42	—	0.03	—	0.07	—	—	0.07
H_2O*	12.14	13.10	13.64	12.30	14.39	11.64	11.64	12.69
Total	100.00	100.00	100.00	100.00	100.00	100.00	100.00	100.00

*Obtained by difference.
n.d. = not determined; — = beyond detection limit.

TABLE VII

Comparison between crystallographic data of Ziemougoula manganite and ASTM manganite

h,k,l	*d* observed	*d* calculated	*d* ASTM No. *8.99*
210	3.3825	3.4116	3.40
301	2.6330	2.6450	2.64
020	2.6330	2.6400	
012	2.5150	2.5215	2.53
202	2.4200	2.4150	2.41
220	2.2675	2.2730	2.28
212	2.1910	2.1960	2.20
420	1.6990	1.7058	1.708
412	1.6640	1.6727	1.672
230	1.6340	1.6376	1.636
032	1.5055	1.5003	1.502
052	1.3200	1.3220	1.326

Calculated parameters:	ASTM *parameters:*
a = 8.925 Å α = 89°53′	a_0 = 8.94 Å α = 90°
b = 5.288 Å β = 90°06′	b_0 = 5.28 Å β = 90°
c = 5.737 Å γ = 90°32′	c_0 = 5.74 Å γ = 90°
V = 270.779 Å^3	V = 270.946 Å^3

MANGANITE FORMATION IN WEATHERED CARBONATE ROCKS OF MOANDA (GABON)

The Precambrian parent-rock of the Moanda minefield is a black calcareous shale which is essentially made up of illite, Mn-bearing carbonates, clusters of pyrite and some detrital silt-size quartz. This shale is also rich in organic matter. Weber (1968), Weber et al. (1979), Boeglin (1981) and Nziengui-Mapangou (1981) have shown that the parent-shale, which outcrops at the base of oxidized profiles, is enriched in rhodochrosite which comes from the subaerial alteration of primary Mg—Ca—Mn-carbonates that are seen in drillcores. Boeglin (1981) gives the following average formulae of these primary carbonates:

$(Mn_{0.64}\,Ca_{0.22}\,Mg_{0.13}\,Fe_{0.01})\,CO_3$ and $(Mn_{0.45}\,Ca_{0.26}\,Mg_{0.29})\,CO_3$

Parent-rock

Thus, the parent-rock consists mainly of rhodochrosite, illite, goethite and quartz. Organic matter always occurs but is much less abundant. The most important mineral is the rhodochrosite. It appears in the rock as ovular micronodules with sharp outlines. The micronodules generally consist of three or four crystals pieced together, but some are monocrystals of rhodochrosite. The matrix between the micronodules is made up of illite, goethite and silt-size quartz. The parent-rock is crossed by fractures, the walls of

TABLE VIII

Chemical composition of the Moanda rhodochrosite

	Sample No.					Average
	1	*2*	*3*	*4*	*5*	
SiO_2	—	0.12	0.70	0.06	0.92	0.36
Al_2O_3	0.07	0.10	0.46	0.02	—	0.13
Fe_2O_3	—	—	—	—	—	—
Cr_2O_3	—	—	—	—	—	—
FeO	0.01	—	0.22	0.03	0.15	0.08
MnO	53.13	55.56	56.65	58.38	55.71	56.29
MgO	0.04	0.06	0.03	0.02	—	0.03
CaO	0.41	0.61	0.27	0.10	0.32	0.34
Na_2O	n.d.	n.d.	n.d.	n.d.	n.d.	n.d.
K_2O	—	0.02	0.08	—	—	0.02
TiO_2	0.01	—	—	—	—	<0.01
CO_2*	44.33	43.53	41.59	41.39	42.90	42.74
Total	100.00	100.00	100.00	100.00	100.00	100.00

*Obtained by difference.
n.d. = not determined; — = beyond detection limit.

PLATE II

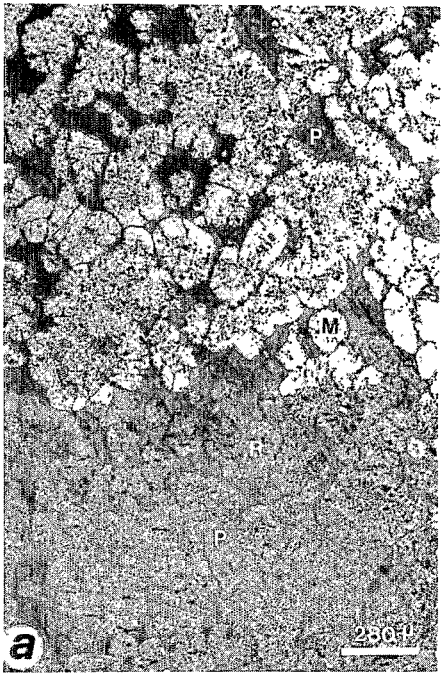

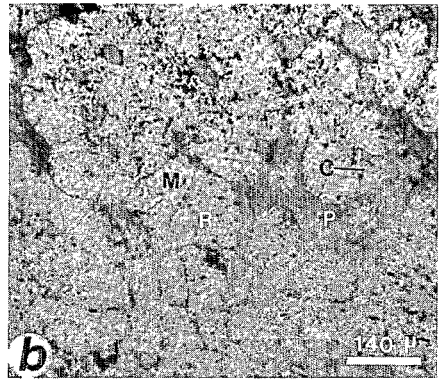

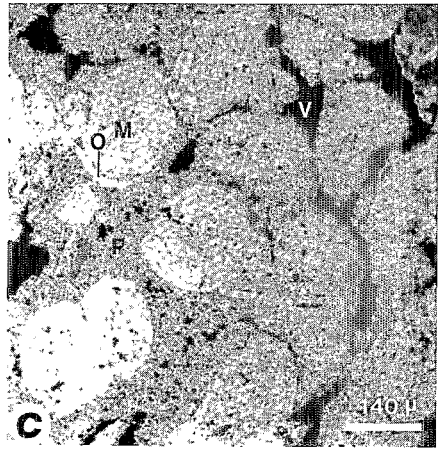

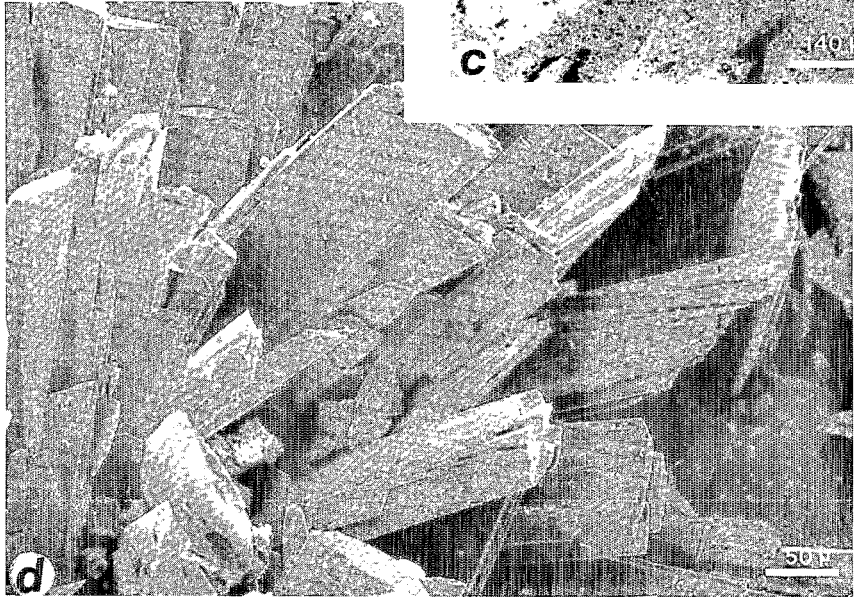

which are coated by very well-crystallized pink rhodochrosite, reaching a few millimetres in size.

There is no difference between the chemical compositions of these well-developed crystals and those of the micronodules. Table VIII gives the chemical composition of the rhodochrosite. The average formula obtained for this parent-mineral is the following:

$(Mn_{0.991}\, Ca_{0.007}\, Fe_{0.001}\, Mg_{0.001})\, CO_3$

Weathering of rhodochrosite into manganite

In the field the boundary between the rhodochrosite-bearing rock and the manganite layer is very clear. This has been noted several times (Bouladon, 1963; Bouladon et al., 1965; Bricker, 1965; Weber, 1968; Perseil and Bouladon, 1971; Weber et al., 1979). This boundary unconformably cuts the thinly bedded parent-shale. Under the microscope (Plate II, a) this boundary is irregular. However, one can still recognize the egg-shaped micronodules, even after they have been transformed into manganite. Locally, the boundary cuts a micronodule, thus demonstrating the development of the manganite at the expense of the rhodochrosite, through pseudomorphic relations (Plate II, b).

The matrix between the manganite micronodules consists mainly of kaolinite and goethite. Illite is scarce and the organic matter has disappeared. Quartz grains are strongly corroded and split into several fragments which keep the crystallographic orientation of the original quartz grain.

In fractures the large crystals of rhodochrosite disappear. Sometimes needle-shaped manganite crystals line the edges of voids (Plate II a). Locally at the base of the profile, one can note around the boundaries of egg-shaped manganite micronodules secondary manganite overgrowths in perfect optical continuity (Plate II, c). It is clear that these overgrowths result from a later precipitation of manganite.

The manganite which replaces the rhodochrosite in micronodules was analysed by the electron microprobe. Chemical compositions are given in

---

PLATE II

Manganite formation in weathering profiles of Moanda (Gabon).

a. Pseudomorphic replacement of rhodochrosite by manganite. R = egg-shaped micronodule of rhodochrosite; M = pseudomorphic manganite; P = argillaceous and ferruginous matrix. Thin section in plain light.

b. Detail of the pseudomorphic replacement of rhodochrosite by manganite. R = rhodochrosite; M = manganite; C = pseudomorphic contact; P = argillaceous and ferruginous matrix. Thin section in plain light.

c. Egg-shaped micronodules of manganite (M) with secondary authigenic overgrowths (O). One can note the development of voids (V) at the expense of the argillaceous and ferruginous matrix (P). Thin section in plain light.

d. Needle-shaped manganite crystals lining the edge of voids. SEM photograph.

TABLE IX

Chemical composition of the manganite of Moanda

	Sample No.								Average
	1	*2*	*3*	*4*	*5*	*6*	*7*	*8*	
SiO_2	0.04	0.08	0.12	0.03	0.38	0.01	0.44	0.47	0.20
Al_2O_3	—	0.16	0.31	0.15	0.17	0.15	—	0.25	0.15
Fe_2O_3	—	—	—	—	—	—	—	—	—
Cr_2O_3	—	0.08	—	—	—	—	0.09	—	0.05
Mn_2O_3	80.98	80.26	82.30	78.97	80.59	80.00	86.61	84.20	81.74
FeO	—	—	—	—	—	—	—	—	—
MgO	0.01	—	—	—	—	—	—	0.02	<0.01
CaO	0.04	—	—	—	—	0.02	—	—	0.01
Na_2O	n.d.	n.d.	n.d.	n.d.	n.d.	n.d.	n.d.	n.d.	n.d.
K_2O	n.d.	n.d.	n.d.	n.d.	n.d.	n.d.	n.d.	n.d.	n.d.
TiO_2	0.04	0.04	—	—	—	—	0.04	—	0.02
H_2O*	18.89	19.38	17.27	20.85	18.86	19.82	12.82	15.06	17.82
Total	100.00	100.00	100.00	100.00	100.00	100.00	100.00	100.00	100.00

*Obtained by difference.
n.d. = not determined; — = beyond detection limit.
Co, Ni, Cu and Zn data are not given in the table as, at this locality, such information is privileged.

TABLE X

Comparison between crystallographic data of Moanda manganite and ASTM manganite

h,k,l	*d* observed	*d* calculated	*d* ASTM No. 8.99
210	3.411	3.4098	3.40
301	2.635	2.6360	2.64
020	2.635	2.6320	
012	2.520	2.5199	2.53
202	2.409	2.4076	2.41
400	2.224	2.2254	2.23
222	1.784	1.7853	1.783
412	1.672	1.6723	1.672
230	1.635	1.6361	1.636
032	1.501	1.5005	1.502
521	1.435	1.4341	1.437

Calculated parameters:	ASTM *parameters:*
a = 8.90 Å α = 89° 34′	a_0 = 8.94 Å α = 90°
b = 5.26 Å β = 89° 52′	b_0 = 5.28 Å β = 90°
c = 5.72 Å γ = 89° 38′	c_0 = 5.74 Å γ = 90°
V = 267.934 Å^3	V = 270.946 Å^3

Table IX. The average formula calculated from these analyses is very near MnOOH.

X-ray characterization of Moanda manganite

The manganite of Moanda was also separated from weathered rock and analysed by XRD. The crystallographic parameters, the unit-cell volume, and the positions of calculated peaks are virtually identical to standard manganite (Table X).

MANGANITE FORMATION IN WEATHERING ENVIRONMENTS

Hewett (1972) concluded that manganite could be hypogene, in veins or in diagenetic stratified bodies, or supergene and generated by weathering of such minerals as rhodochrosite $MnCO_3$ and rhodonite $MnSiO_3$. It would be difficult to review the entire literature concerning manganite γ-MnOOH generated in supergene conditions. However, through examples chosen in the tropical and equatorial zone, one can note that manganite is effectively generated from the weathering of rhodochrosite, as in Africa at Nsuta (Perseil and Grandin, 1978), at Moanda (Perseil and Bouladon, 1971) or as in Brazil at Conselheiro Lafaiete (Horen, 1953; Bittencourt, 1973). Furthermore, manganite appears as the weathering product of Mn-pyroxenoids and Mn-garnets (Bittencourt, 1973).

Experimental weathering, under lateritic conditions, of a rock made up of 75% pyroxmangite, 8% rhodonite and 6% rhodochrosite, Mn-amphibole and serpentine reveals that well-crystallized and stoichiometric oxyhydroxides such as manganite and groutite appear in the first stage of weathering (Melfi et al., 1973; Melfi and Pedro, 1974). Manganite indeed occurs in weathering profiles, not only as replacement of parent-minerals but also as authigenic needle-shaped crystals in voids and fissures. Such a phenomenon was noted at Nsuta (Perseil and Grandin, 1978) and at Moanda. Moreover, at Moanda we have described secondary authigenic overgrowths of manganite.

Manganite has been noted in lateritic profiles without references to the possible parent-mineral (Roy, 1968; Eswaran and Raghu Mohan, 1973). Manganite is generally not found to be an abundant phase when generated by supergene oxidation of pre-existing manganese minerals. In the two African examples which we have studied in minute detail, manganite occurs as millimetre- or centimetre-thick layers at the base of profiles 10—12 m thick. In weathering environments the geochemical conditions of manganite formation are limited. It may be preceded by hausmannite ((MnO, Mn_2O_3)) formation at the expense of parent-mineral, or the manganite may be followed by the formation of birnessite, cryptomelane, nsutite and pyrolusite (Roy, 1968). The limited stability field of manganite is corroborated by the thermodynamic data. Some values of the free energy of formation ΔF^0_f were determined for manganite, γ-MnOOH, by Drotschmann (1951), Wadsley and

Walkley (1951), Latimer (1952) and Bode et al. (1962). The results obtained by different methods are all between −557.5 and −571.5 kJ mol^{-1}. Hem (1963, 1972, 1978), Garrels and Christ (1965) and Bricker (1965) generally take $\Delta F^0_f = -557.7$ kJ mol^{-1} for plotting stability fields of the different Mn-oxyhydroxides in pH—Eh diagrams. Manganite appears as an intermediate mineral between hausmannite and pyrolusite β-MnO_2. In fact, the other "dioxides", such as birnessite, cryptomelane or nsutite are rarely considered in that type of diagram, because of their variable thermodynamic values. Manganite may only exist in a pH region > 7.5 (at 25°C and 1 atm, for log $[Mn^{2+}] = -6.00$); its interval of stability, in Eh terms, is 0.15 V wide, for Eh < 0.55 V. When the fugacity of CO_2 is high (log $f_{CO_2} = -2.5$ vs. −3.5 in the "normal" atmosphere), the stability field of haumannite is completely covered by that of rhodochrosite $MnCO_3$. In a log f_{O_2} vs. log $[Mn^{2+}]/[H^+]^2$ diagram, Boeglin (1981) shows that the field of manganite, between rhodochrosite and pyrolusite, is limited between log $f_{O_2} = -23$ (for log $[Mn^{2+}]/[H^+]^2 = 10.4$) and log $f_{O_2} = -18$ (for log $[Mn^{2+}]/[H^+]^2 = 9.3$). Thus, manganite appears as a transition phase between the carbonate of reducing environments and the dioxides of oxidizing environments.

Except for very large and well-crystallized manganite of hypogene origin (Hewett 1972), the literature does not give precise chemical analyses for manganite originating by weathering. With the electron microprobe we can show that: (1) the chemical composition of manganite is different for different parent-material; (2) manganite crystallizes in microenvironments where foreign elements, such as Si, Ca and Mg, are present in weathering solutions; and (3) the purest manganite crystals are located in veins, cracks or fissures. In fact, in weathering profiles, in a single layer of few millimetres to few centimetres thick, i.e. in a single chemical environment, manganite appears as the stable Mn-oxyhydroxide. Each Mn-bearing parent-mineral (carbonate or silicate) being unstable to weathering will be transformed into manganite. Mn-garnets will react to weathering solutions higher in the profile. The persistence and greater duration of oxidative drainage in the upper part of the profile creates a zone in which Mn^{4+} is stable. In this zone manganite is no longer stable and converts to birnessite and lithiophorite, and the spessartite garnet is also converted to these phases. Thus, the stability of manganite is limited to a layer a few millimetres or a few centimetres thick in weathering profiles.

In view of the compositional contrasts among the various parent-minerals of the manganites described and analysed here, it is of interest to explore the possibility of distinguishing manganites of different parageneses. The MnO/(CaO + MgO) diagram (Fig. 1) shows that manganite crystals originating from manganocalcite are chemically different from those originating from tephroite or from rhodochrosite, even if these parent-minerals are merely separated by a grain-boundary fracture. Each parent carbonate or silicate mineral is pseudomorphically replaced by manganite. This process of replacement includes both dissolution of the parent-mineral and precipitation

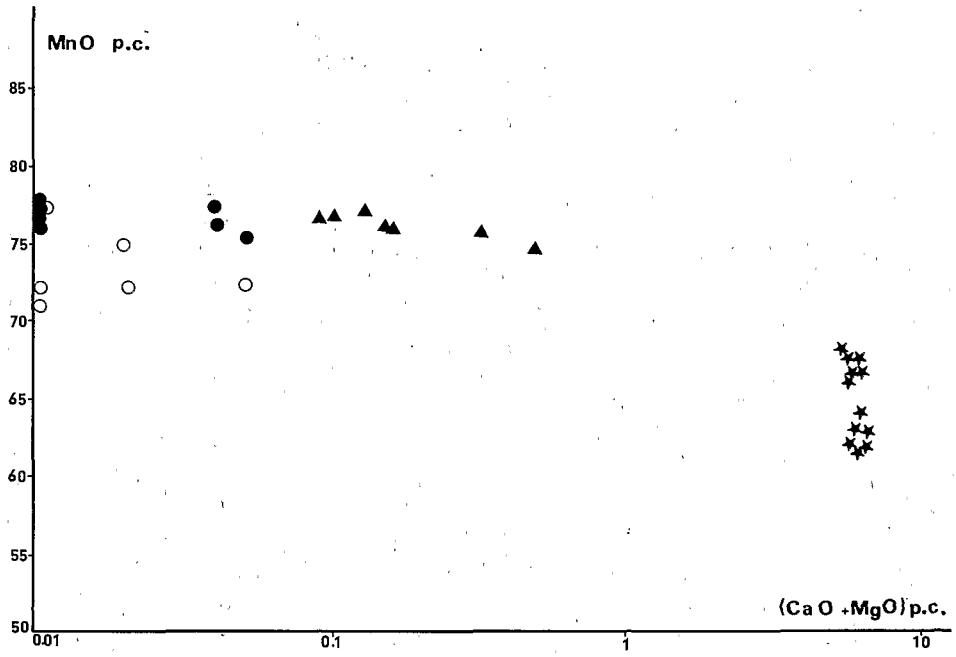

Fig. 1. The MnO/(CaO + MgO) diagram of manganites. ★ = Manganites from manganocalcites of Ziemougoula; ▲ = manganites from tephroites of Ziemougoula; ● = manganites in microfissures (Ziemougoula); ○ = manganites of Moanda.

of the new Mn^{3+} phase. It is essentially congruent initially, but some of the Ca, Mg and Si (and other transition metals) is trapped and is either adsorbed to manganite crystals (this is suggested for Mg and Ca in Fig. 1) or reconcentrated into microsilicifications. Thus, with advanced and pseudomorphic replacement the complete flushing of the unincorporated elements has not been effected. However, in the manganite crystals which line fissures and are clearly due to crystallization from solution, we have an instance of the composition of the almost pure manganite. This is probably owing to an increased rate of flushing of the rock by water in larger fissures.

Microprobe data clearly show that SiO_2 is extra-structural and occurs in microsilicifications. The uniform distribution of Mg and Ca in microprobe analysis would appear to indicate that these latter elements are incorporated in the structure of manganite. A number of lines of evidence dictate otherwise: (1) X-ray data and optical examination show no difference between manganites of fissure-filling or pseudomorphic origins; (2) the fissure-manganite is relatively free of Ca and Mg; (3) because of the coordination number, the valence and ionic radius, it is impossible to consider a substitution for Mn^{3+}. Thus, all these dictate dispersion by adsorption on surfaces of growing manganite minerals.

In fact, through the studies of Dachs (1963), Bricker (1965), Giovanoli and Stähli (1970), Giovanoli et al. (1971) and Burns and Burns (1975), we know that Mn^{3+} occupies the centre of octahedrons which consist of oxygen and hydroxyl. The octahedrons are developed into chains along the *C*-axis to form monoclinic crystallo-orthorhombic crystals. From the values of crystallographic parameters obtained on the manganites of Ziemougoula and Moanda (Tables VII and X), one could estimate the deformation of the structural (MnO_6) octahedron as a function of the formal oxidization rate of Mn (Jahn—Teller effect, Giovanoli and Leuenberger, 1969). We could calculate that the analysed manganite of both areas consists of Mn^{3+}. Thus, except for Fe^{3+}, a substitution for Mn^{3+} is impossible. Murray (1975) concluded that selective adsorption of transition-metal ions and alkaline-earth-metal ions takes place on the surface of hydrous manganese dioxide. The transition-metal ions, principally Co^{2+}, have a greater attraction than the alkaline-earth metals, and for these latter, Ca^{2+} is fixed more than Mg^{2+}. Burns (1976) proposes that Co^{2+} may initially be adsorbed on to the surface of some Mn^{4+}-oxides and then it is oxidized into Co^{3+} and substitutes for Mn^{4+} ions in "edge-shared [MnO_6] octahedra". Through the two examples presented in this paper, we can corroborate the results obtained by Murray (1975). Microprobe chemical analyses of manganites show a greater concentration of Ca with regard to Mg, even though the parent-mineral is richer in Mg. This certainly proves: (1) an adsorption on oxyhydroxide manganese surfaces of alkaline-earth metals released from parent-minerals by the weathering process; (2) a greater attraction of Ca^{2+} for Mn-oxyhydroxide. Moreover, in the latest manganites, i.e. in manganites which crystallize in environments where the leaching of cations is more important (manganite of fissures and cracks), Mg^{2+} and Ca^{2+} are almost entirely released. On the other hand, the behaviour of Co is different. Along with Fe, which is probably substituted for Mn^{3+}, Co is enriched. This proves: (1) either that Co presents a higher degree of adsorption on Mn^{3+}-oxyhydroxide; or (2) that Co^{3+} may substitute for Mn^{3+}; this latter proposition is considered by Burns (1976) as unsatisfactory.

ACKNOWLEDGEMENTS

The authors are indebted to the SODEMI Company (Ivory Coast) and COMILOG (Gabon) for their generous cooperation. They also are grateful to Drs. E.A. Perseil, F. Weber and Y. Tardy for their help and suggestions, to Dr. Z.S. Altschuler and Dr. Giovanoli for the helpful review of an earlier draft. They also thank C. Augas and B. Braconnier for their technical assistance. SEM photographs are by courtesy of JEOL, Paris.

REFERENCES

Bittencourt, A.V., 1973. Contribuçao as estudo genetico do minerio de manganes de Conselheiro Lafaiete. Minas Gerais. Thesis, University of São Paulo, São Paulo (unpublished).

Bode, H., Schmier, A. and Berndt, D., 1962. Zur Phasenanalyse von Mangandioxyd. Z. Elektrochem., 66: 586—593.

Boeglin, J.L., 1981. Minéralogie et géochimie des gisements de manganèse de Conselheiro Lafaiete au Brésil et de Moanda au Gabon. Thesis, University of Toulouse, Toulouse (unpublished).

Bouladon, J., 1963. Le gisement de manganèse de Moanda (Gabon) — Étude de la zone de première exploitation. Bur. Rech. Géol. Min. (B.R.G.M.), Rép. No. 5313 (unpublished).

Bouladon, J., Weber, F., Veysset, C. and Favre-Mercuret, R., 1965. Sur la situation géologique et le type métallogénique du gisement de manganèse de Moanda près de Franceville (Rép. gabonaise). Serv. Carte Géol. Alsace—Lorraine, Bull., 18: 253—276.

Bricker, O., 1965. Some stability relations in the system $Mn—O_2—H_2O$ at 25° and one atmosphere total pressure. Am. Mineral., 50: 1296—1354.

Burns, R.G., 1976. The uptake of cobalt into ferromanganese nodules, soils, and synthetic manganese(IV) oxides. Geochim. Cosmochim. Acta, 40: 95—102.

Burns, R.G. and Burns, V.M., 1975. Structural relationships between the manganese(IV) oxides. In: A. Kozawa and R.J. Brodd (Editors), Proc. Int. Symp. Manganese Dioxides, Cleveland, Ohio, pp. 306—327.

Dachs, H., 1963. Neutron- und Röntgenuntersuchungen am Manganit. Z. Kristallogr. Mineral., 118: 303—326.

Drotschmann, C., 1951. Moderne Primarbatterien. S. 10, N. Brantz (Editor).

Eswaran, H. and Raghu Mohan, N.G., 1973. The microfabric of petrolinthite. Soil Sci. Soc. Am. Proc., 37: 79—82.

Garrels, R.M. and Christ, C.L., 1965. Solutions, Minerals and Equilibria. Freeman Cooper, San Francisco, Calif., 450 pp.

Giovanoli, R. and Leuenberger, U., 1969. Uber die Oxydation von Manganoxidhydroxid. Helv. Chim. Acta, 52: 2333—2357.

Giovanoli, R. and Stähli, E., 1970. Oxide und Oxidhydroxide des drei- und vierwertigen Mangans. Chimia, 24: 49—61.

Giovanoli, R., Feitknecht, W. and Fischer, F., 1971. Über Oxidhydroxide des vierwertigen Mangans mit Schichtengitten, 3. Mitteilung: Reduktion von Mangan(III) — Manganat(IV) mit Zimtalkohol. Helv. Chim. Acta, 54: 1112—1124.

Hem, J.D., 1963. Chemical equilibria and rates of manganese oxidation. U.S. Geol. Surv., Water-Supply Pap. 1667-A, 64 pp.

Hem, J.D., 1972. Chemical factors that influence the availability of iron and manganese in aqueous system. Geol. Soc. Am., Spec. Pap., 140: 17—24.

Hem, J.D., 1978. Redox processes at surfaces of manganese oxide and their effects on aqueous metal ions. Chem. Geol., 21: 199—218.

Hewett, D.F., 1972. Manganite, hausmannite, braunite: features, modes of origin. Econ. Geol., 67: 83—102.

Horen, A., 1953. The manganese mineralizations at the Merid-Mine, Minais-Gerais, Brazil. Ph.D. Thesis, Harvard University, Cambridge, Mass. (unpublished).

Latimer, W.M., 1952. Oxidation Potentials. Prentice-Hall, Englewood Cliffs, N.J.

Melfi, A.J. and Pedro, G., 1974. Étude sur l'altération expérimentale de silicates manganésifères et la formation exogène des gisements de manganèse. Groupe Fr. Argiles, Bull., 26: 91—105.

Melfi, A.J., Valarelli, J.V., Pedro, G., Levi, F. and Hypolito, R., 1973. Étude sur la formation d'oxydes et d'hydroxydes de manganèse par altération expérimentale de silicates manganésifères. C.R. Acad. Sci. Paris, Sér. D, 277: 5—8.

Murray, J.W., 1975. The interaction of metal ions at the manganese dioxide—solution interface. Geochim. Cosmochim. Acta, 39: 505—519.

Nahon, D., Colin, F. and Tardy, Y., 1982. Formation and distribution of Mg, Fe, Mn-smectites in the first stages of the lateritic weathering of forsterite and tephroite. Clay Miner., 17: 339—348.

Nziengui-Mapangou, P., 1981. Pétrologie comparée de gisements manganésifères supergènes en Afrique (gisement de Ziémougoula en Côte d'Ivoire et gisement de Moanda au Gabon). Thesis, University of Poitiers, Poitiers (unpublished).

Perseil, E.A. and Bouladon, J., 1971. Microstructures des oxydes de manganèse à la base du gisement de Moanda (Gabon) et leur signification génétique. C.R. Acad. Sci. Paris, Sér. D., 273: 278—279.

Perseil, E.A. and Grandin, G., 1978. Évolution minéralogique du manganèse dans trois gisements d'Afrique de l'Ouest: Mokta, Tambao, Nsuta. Miner. Deposita, 13: 295—311.

Roy, S., 1968. Mineralogy of the different genetic types of manganese deposits. Econ. Geol., 63: 760—786.

Wadsley, A.D. and Walkley, A., 1951. The structure and reactivity of the oxides of manganese. Rev. Pure Appl. Chem., 1: 203—213.

Weber, F., 1968. Une série précambrienne du Gabon: Le Francevillien. Sédimentologie, géochimie, relations avec les gîtes minéraux associés. Mém. Serv. Carte Géol. Alsace—Lorraine, 28, 328 pp.

Weber, F., Leclerc, J. and Millot, G., 1979. Epigénies manganésifères successives dans le gisement de Moanda (Gabon). Sci. Géol., Bull., 32: 147—164.